Journal of Sound and Vibration (2002) **257**(1), 107–117
doi:10.1006/jsvi.5033, available online at http://www.idealibrary.com on IDEAL®

DYNAMIC RESPONSE OF A ROTATING FLEXIBLE ARM CARRYING A MOVING MASS

D. T. W. YAU AND E. H. K. FUNG

Department of Mechanical Engineering, The Hong Kong Polytechnic University, Hung Hom, Kowloon, Hong Kong, People's Republic of China. E-mail: mmhkfung@polyu.edu.hk

(*Received* 4 *June* 2001, *and in final form* 11 *February* 2002)

A clamped–free flexible arm rotating in a horizontal plane and carrying a moving mass is studied in this paper. The arm is modelled by the Euler–Bernoulli beam theory in which rotatory inertia and shear deformation effects are ignored. The assumed mode method in conjunction with Hamilton's principle is used to derive the equation of motion of the system which takes into account the effect of centrifugal stiffening due to the rotation of the beam. The eigenfunctions of a cantilever beam which satisfy the prescribed geometric boundary conditions are used as basis functions in the assumed mode method. The equation of motion is expressed in non-dimensional matrix form. Pre-designed transformed cosine profiles are used as trajectory inputs for the hub angle and the moving mass. The equation of motion is solved numerically using the fourth order Runge–Kutta method. Graphical results are presented to show the influence of centrifugal stiffening effect, moving mass values, mass travelling time, hub angle and mass trajectory profile on the deflection of the beam.

© 2002 Elsevier Science Ltd. All rights reserved.

1. INTRODUCTION

The vibration behaviour of a flexible beam subjected to moving mass has long been an important subject for investigation as it finds many practical applications such as bridges on which vehicles or trains travel, and a robotic arm carrying a moving end effector.

The above problem is usually modelled by a non-rotating simply supported or clamped-free cantilever beam acted upon by a moving force [1, 2] or a moving mass [3–12]. Most researchers investigated the effects of different mass position, mass travelling velocity and mass inertia on the vibration behaviour of the beam [3–7]. Some others compared the difference between the moving force model and the moving mass model [8]. Lee [8] studied the dynamic response of a clamped–clamped beam acted upon by a moving mass. He analyzed the problem of the moving mass separating from the beam by monitoring the contact forces between them. He also showed that the "moving-force" formulation is not always an upper bound solution for the corresponding "moving-force moving-mass" formulation. Stanisic [10] developed a method to obtain mode shapes which account for the motion of the mass by dividing the beam into two separate regions with respect to the moving mass. Recently, Park *et al.* [12] investigated the vibration behaviour of an elastic beam fixed on a moving cart and carrying a moving mass.

In all the above studies the beam under investigation is considered to be non-rotating. Fung *et al.* [13] investigated the vibration frequencies of a rotating flexible arm carrying a moving mass which takes into account the effect of centrifugal stiffening [14] due to the rotation of the arm. The present study extends the work of reference [13] to investigate the

0022-460X/02/$35.00 © 2002 Elsevier Science Ltd. All rights reserved.

dynamic response of the same system. The effect of centrifugal stiffening due to the rotation of the arm is also taken into account in the investigation. The arm is rotating in a horizontal plane in which the gravitational effect is neglected. The assumed mode method in conjunction with Hamiltion's principle is used to derive the equation of motion of the system. The trajectories of the hub angle and the moving mass are simulated using pre-designed transformed cosine profiles. The equation of motion is solved numerically and the results show the influence of centrifugal stiffening effect, moving mass values, mass travelling time, hub angle and mass trajectory profile on the deflection of the beam.

2. THEORY AND FORMULATION

Figure 1 shows a flexible arm modelled by the Euler–Bernoulli beam theory rotates at an angular velocity of $\dot{\theta}$ in a horizontal plane about the clamped axis and has a mass m travelling along it. The arm is of length L, mass per unit length ρ and flexural rigidity EI. Let OXY and Oij represent the inertial and rotating Cartesian axes respectively. The mass moment of inertia of the hub is J. The transverse displacement of a spatial point on the beam at a distance r $(0<r<L)$ from the origin is denoted by $w(r,t)$ while the velocity of the moving mass relative to the beam is denoted by $\dot{s}(t)$. The position vector $\mathbf{r}$ at a spatial position r and the resultant velocity $\mathbf{V}_m$ of the mass are given by

$$\mathbf{r} = r\mathbf{i} - w(r,t)\mathbf{j}, \qquad \dot{\mathbf{r}} = w(r,t)\dot{\theta}\mathbf{i} + r\dot{\theta}\mathbf{j} - \dot{w}(r,t)\mathbf{j}, \tag{1}$$

$$\mathbf{V}_m = [\dot{\mathbf{r}} + \dot{\mathbf{s}}]_{r=s} = [(\dot{s} + w\dot{\theta})\mathbf{i} + (r\dot{\theta} - \dot{w} - \dot{s}w')\mathbf{j}]_{r=s}, \tag{2}$$

where a dot and a prime denote the derivatives with respect to time t and the spatial variable r respectively. The kinetic energy of the beam T_b, the kinetic energy of the moving mass T_m, the total potential energy of the system V and the virtual work done δW by the local driving force for the moving mass F_m and the applied hub torque τ are given by

$$\begin{aligned} T_b &= \frac{1}{2}\int_0^L \rho\dot{\mathbf{r}}^{\mathrm{T}}\dot{\mathbf{r}}\,\mathrm{d}r + \frac{1}{2}J\dot{\theta}^2 \\ &= \frac{1}{2}\int_0^L \rho(w^2\dot{\theta}^2 + r^2\dot{\theta}^2 + \dot{w}^2 - 2r\dot{\theta}\dot{w})\,\mathrm{d}r + \frac{1}{2}J\dot{\theta}^2, \end{aligned} \tag{3}$$

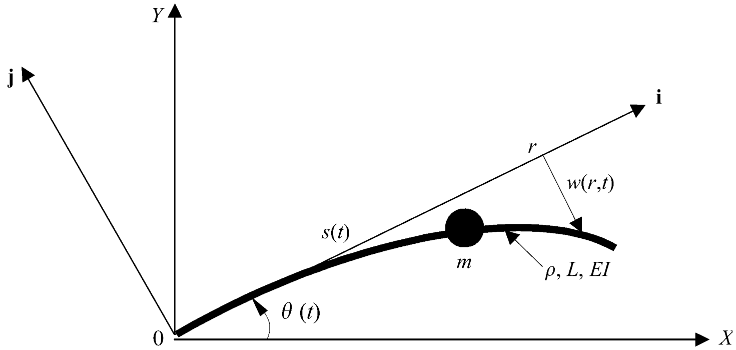

Figure 1. A rotating flexible arm carrying a moving mass.

$$T_m = \frac{1}{2} m \mathbf{V}_m^{\mathrm{T}} \mathbf{V}_m$$
$$= \frac{1}{2} m [\dot{s}^2 (1 + w'^2) + 2\dot{s}(\dot{w}w' - r\dot{\theta}w' + \dot{\theta}w) + \dot{\theta}^2 w^2 + (r\dot{\theta} - \dot{w})^2]_{r=s}, \tag{4}$$

$$V = \frac{EI}{2} \int_0^L w''^2 \, \mathrm{d}r + \frac{1}{2} \int_0^L P(r,t) w'^2 \, \mathrm{d}r, \quad \delta W = F_m \, \delta s + \tau \delta\theta, \tag{5, 6}$$

where $P(r,t)$ is the centrifugal force due to the centrifugal stiffening effect [14] given by

$$P(r,t) = \begin{cases} ms\dot{\theta}^2 + \int_r^L \rho r \dot{\theta}^2 \, \mathrm{d}r, & 0 \leqslant r \leqslant s, \\ \int_r^L \rho r \dot{\theta}^2 \, \mathrm{d}r, & s < r \leqslant L. \end{cases} \tag{7}$$

By applying Hamilton's principle,

$$\int_{t_1}^{t_2} (\delta T_b + \delta T_m - \delta V + \delta W) \, \mathrm{d}t = 0 \tag{8}$$

and considering only those terms related to δw, the governing equation of motion of the flexible beam can be obtained. The non-dimensional parameters are defined as follows:

$$\xi = \frac{r}{L}, \qquad s_0 = \frac{s}{L}, \qquad N = \frac{m}{\rho L},$$
$$v = \frac{w}{L}, \qquad T = \frac{t}{L^2}\sqrt{\frac{EI}{\rho}}, \qquad \eta = \sqrt{\frac{\rho}{EI}}\dot{\theta}L^2. \tag{9}$$

By using the assumed mode method, the non-dimensional transverse deflection $v(\xi, T)$ of the beam is expressed as

$$v(\xi, T) = \sum_{i=1}^{n} Y_i(\xi) q_i(T), \tag{10}$$

where $Y_i(\xi)$ are the mode shape functions or eigenfunctions and $q_i(T)$ are the generalized co-ordinates which are unknown functions of time.

Substituting equations (9) and (10) into equations (3)–(8), and considering only those terms related to δq_i the non-dimensional equation of motion of the flexible beam is obtained and is expressed in matrix form as:

$$(\mathbf{M} + N\mathbf{H})\ddot{\mathbf{q}} + N\dot{s}_0(\mathbf{B} - \mathbf{C})\dot{\mathbf{q}} + [\mathbf{K} - \eta^2\mathbf{M} + N(\ddot{s}_0\mathbf{B} - \dot{s}_0^2\mathbf{A} - \eta^2\mathbf{H})]\mathbf{q}$$
$$= \dot{\eta}\mathbf{\Phi} - Ns_0\dot{s}_0\eta\mathbf{Y}' + N(\dot{s}_0\eta + s_0\dot{\eta})\mathbf{Y}, \tag{11}$$

where a dot and a prime denote the derivatives with respect to the non-dimensional time T and spatial variable ξ respectively, and

$$\mathbf{A} = [Y_i'(s_0)\, Y_j'(s_0)], \quad \mathbf{B} = [Y_i(s_0)\, Y_j'(s_0)], \quad \mathbf{C} = [Y_i'(s_0)\, Y_j(s_0)] \quad i,j = 1, 2, \ldots, n, \tag{12−14}$$

$$\mathbf{H} = [Y_i(s_0)\, Y_j(s_0)], \quad \mathbf{M} = \left[\int_0^1 Y_i(\xi)\, Y_j(\xi) \, \mathrm{d}\xi\right], \quad i,j = 1, 2, \ldots, n, \tag{15, 16}$$

$$\mathbf{K} = \left[\int_0^1 \{Y_i''(\xi)\, Y_j''(\xi) + P_0(\xi)\, Y_i'(\xi)\, Y_j'(\xi)\} \, \mathrm{d}\xi\right], \quad i,j, = 1, 2, \ldots, n, \tag{17}$$

$$\mathbf{\Phi} = \left\{\int_0^1 \xi Y_i(\xi) \, \mathrm{d}\xi\right\}^{\mathrm{T}}, \quad \mathbf{Y} = \{Y_i(s_0)\}^{\mathrm{T}}, \quad \mathbf{q} = \{q_i(T)\}^{\mathrm{T}}, \quad i = 1, 2, \ldots, n, \tag{18−20}$$

$$P_0(\xi) = \begin{cases} Ns_0\eta^2 + \dfrac{1}{2}\eta^2(1-\xi^2), & 0 \leqslant \xi \leqslant s_0, \\ \dfrac{1}{2}\eta^2(1-\xi^2), & s_0 < \xi \leqslant 1. \end{cases} \tag{21}$$

The initial conditions of equation (11) are assumed to be $\mathbf{q}(0) = \dot{\mathbf{q}}(0) = 0$.

3. NUMERICAL SIMULATION

In this paper, the eigenfunctions of a non-rotating cantilever beam [9] is chosen as the mode shape in equation (10) and is given by

$$Y_i(\xi) = \cosh(k_i\xi) - \cos(k_i\xi) - \frac{\cos(k_i) + \cosh(k_i)}{\sin(k_i) + \sinh(k_i)}(\sinh(k_i\xi) - \sin(k_i\xi)) \quad i = 1, 2, 3, \ldots. \tag{22}$$

These eigenfunctions do not represent the exact mode shape of the complete system since they do not account for the effects of the moving mass F_m and the centrifugal stiffening due to the rotation of the beam. However, they are selected in this paper because of their orthogonal property and also they satisfy the geometric boundary conditions of the system [9]. In this paper, only the first three modes are considered. The frequency parameters k_i in equation (22) have the values

$$k_1 = 1{\cdot}8751, \quad k_2 = 4{\cdot}6941 \quad \text{and} \quad k_3 = 7{\cdot}8548.$$

In order to perform numerical simulation for the rotating flexible beam under the moving mass, the local driving force for the moving mass F_m and the applied hub torque τ are pre-designed [12] to generate transformed cosine trajectory profiles for the moving mass and the hub angle (Figure 2). This profile provides zero velocity and acceleration at both the initial and final positions of the moving mass. The profile thus chosen for the hub angle and the moving mass are given by

$$\eta = \frac{f(T)\dot{g}(T) - \dot{f}(T)g(T)}{f^2(T) + g^2(T)}, \quad \dot{s}_0 = \frac{f(T)\dot{f}(T) + g(T)\dot{g}(T)}{[f^2(T) + g^2(T)]^{0{\cdot}5}}, \tag{23, 24}$$

where

$$f(T) = \begin{cases} x_1 + \dfrac{x_2 - x_1}{T_t}\left[T - \dfrac{T_t}{2\pi}\sin\left(\dfrac{2\pi T}{T_t}\right)\right], & 0 \leqslant T < T_t, \\ x_2, & T \geqslant T_t, \end{cases} \tag{25}$$

$$g(T) = \begin{cases} y_1 + \dfrac{y_2 - y_1}{T_t}\left[T - \dfrac{T_t}{2\pi}\sin\left(\dfrac{2\pi T}{T_t}\right)\right], & 0 \leqslant T < T_t, \\ y_2, & T \geqslant T_t \end{cases} \tag{26}$$

and (x_1, y_1) and (x_2, y_2) are the initial and final positions of the moving mass with reference to the axes OXY respectively, and T_t is the travelling time of the mass. If the beam flexibility is negligible, the trajectory described by the moving mass is a straight line in the inertial frame, and the resulting velocity and acceleration profiles can also be described by the transformed cosines.

In the present simulation, two cases with different initial and final positions of the moving mass are used. In case 1 the mass is moved towards the free end from (0·025, 0·2) to (0·8, 0·1), whereas in case 2 the mass is moved towards the clamped end from (0·8, 0·1) to (0·025, 0·2). In both cases, the total non-dimensional simulation time is 25. The mass

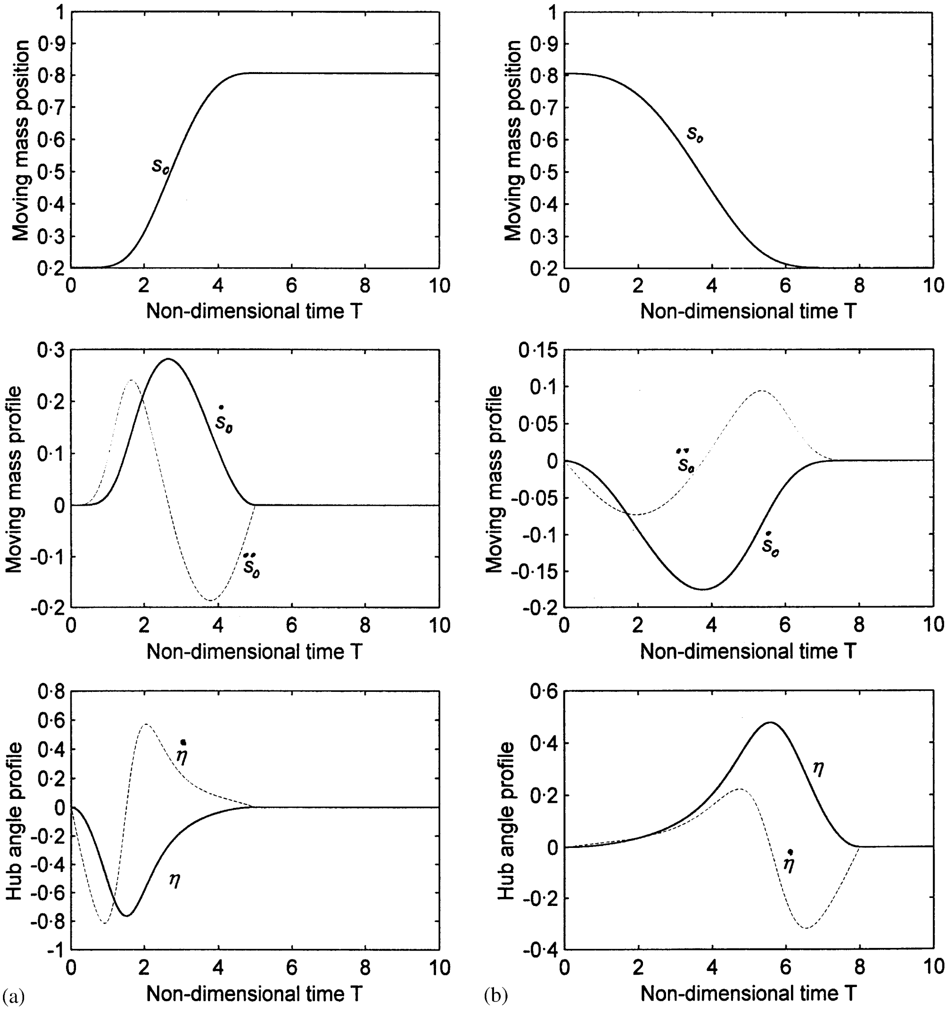

Figure 2. Moving mass and hub angle trajectory profiles. (a) case 1, $T_t = 5$; (b) case 2, $T_t = 8$.

travelling time T_t in each case is varied from 5 to 8 while the mass value N is varied from 0·5 to 2.

After the travelling time T_t has passed ($T \geqslant T_t$), there is no mass and beam motion, i.e., $\dot{s}_0$, $\ddot{s}_0$, η and $\dot{\eta}$ are all zero. The system is in the steady state and the equation of motion (11) is reduced to homogeneous second order ordinary differential equations as follows:

$$(\mathbf{M} + N\mathbf{H})\ddot{\mathbf{q}} + \mathbf{K}\mathbf{q} = 0. \tag{27}$$

4. RESULTS

Upon substituting the hub angle and the moving mass trajectory profiles [equations (23)–(26)] into the equation of motion of the system (11), the fourth order Runge–Kutta method in conjunction with MATLAB is used to obtain the numerical results of the beam deflection under different values of moving mass N and mass travelling time T_t.

Figures 3–8 show the non-dimensional deflection of the beam at the position of the moving mass $v(s_0, T)$ plotted against the non-dimensional time T under different values of

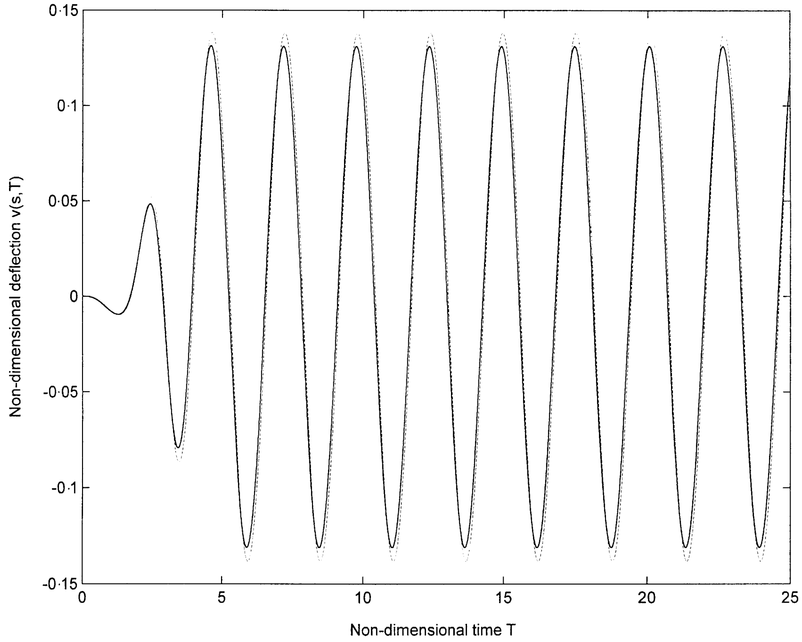

Figure 3. Non-dimensional deflection of beam under the moving mass $v(s_0, T)$ for $N = 0{\cdot}5$ and $T_t = 5$ in case 1 (mass is moved towards the free end): ——, with centrifugal stiffening effect; - - -, without centrifugal stiffening effect.

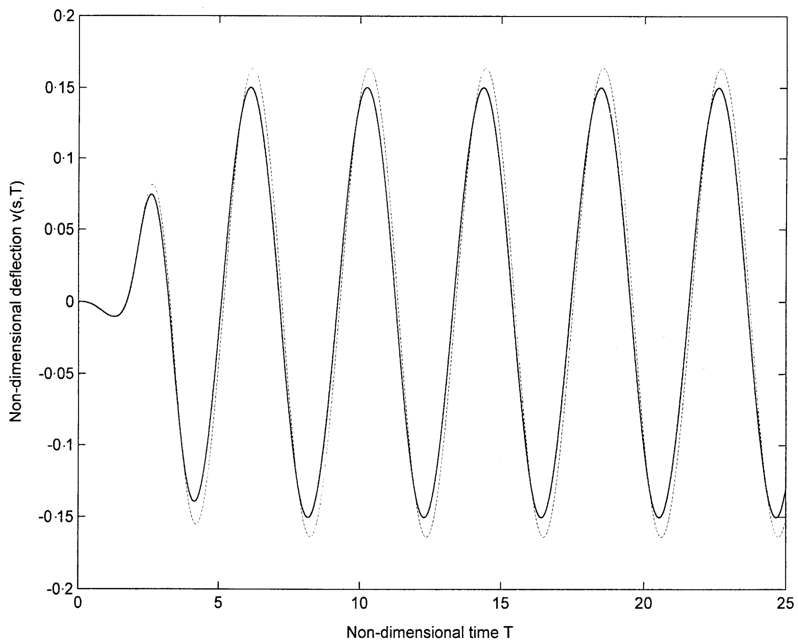

Figure 4. Non-dimensional deflection of beam under the moving mass $v(s_0, T)$ for $N = 2{\cdot}0$ and $T_t = 5$ in case 1 (mass is moved towards the free end): ——, with centrifugal stiffening effect; - - -, without centrifugal stiffening effect.

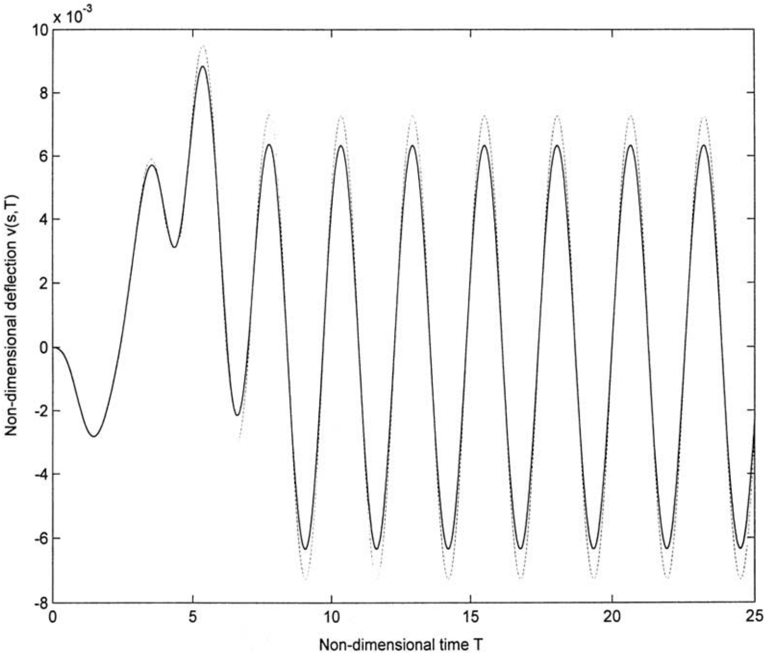

Figure 5. Non-dimensional deflection of beam under the moving mass $v(s_0, T)$ for $N = 0{\cdot}5$ and $T_t = 8$ in case 1 (mass is moved towards the free end): ——, with centrifugal stiffening effect; - - -, without centrifugal stiffening effect.

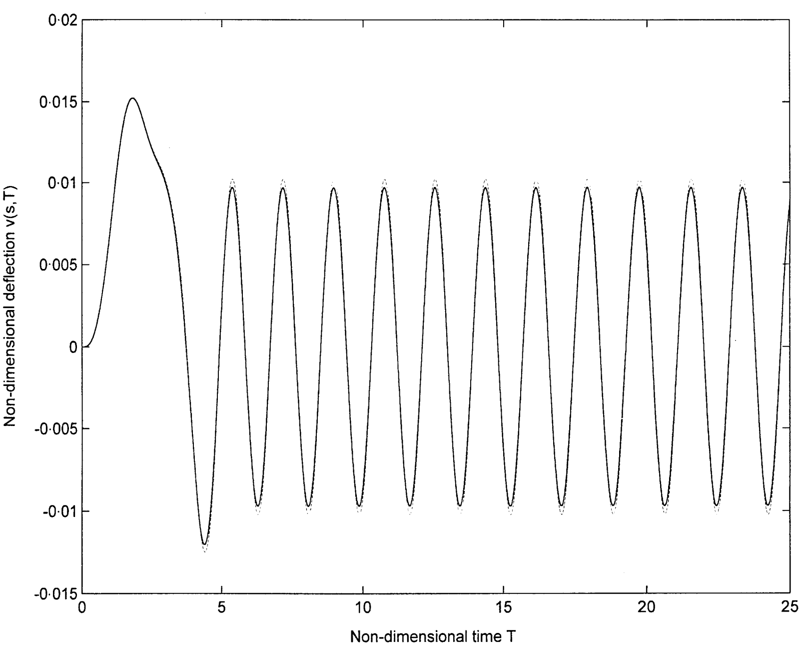

Figure 6. Non-dimensional deflection of beam under the moving mass $v(s_0, T)$ for $N = 0{\cdot}5$ and $T_t = 5$ in case 2 (mass is moved towards the clamped end): ——, with centrifugal stiffening effect; - - -, without centrifugal stiffening effect.

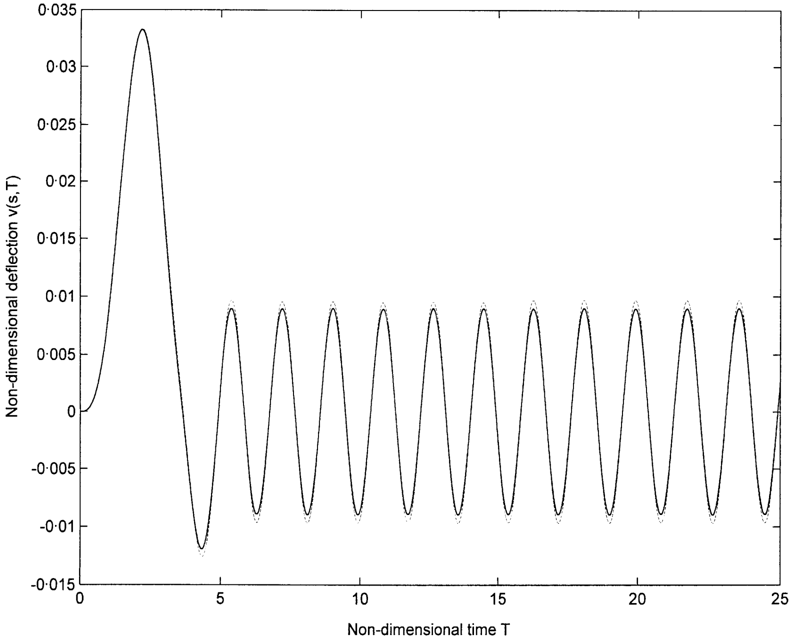

Figure 7. Non-dimensional deflection of beam under the moving mass $v(s_0, T)$ for $N = 2{\cdot}0$ and $T_t = 5$ in case 2 (mass is moved towards the clamped end): ——, with centrifugal stiffening effect; - - -, without centrifugal stiffening effect.

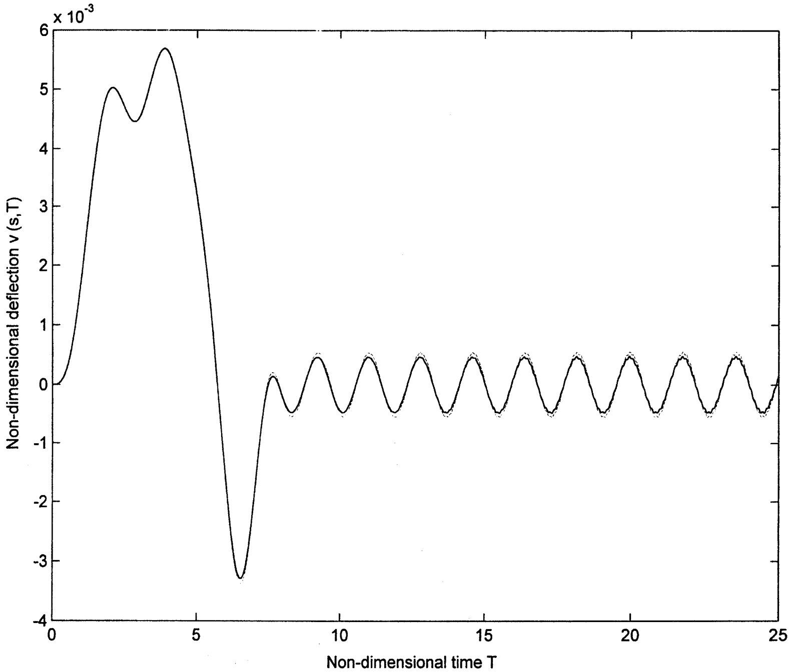

Figure 8. Non-dimensional deflection of beam under the moving mass $v(s_0, T)$ for $N = 0{\cdot}5$ and $T_t = 8$ in case 2 (mass is moved towards the clamped end): ——, with centrifugal stiffening effect; - - -, without centrifugal stiffening effect.

moving mass N and mass travelling time T_t for cases 1 and 2. Comparison of the first and second peak deflections in the transient state ($0 \leqslant T < T_t$) show that in case 1 (the mass is moved towards the free end) the first peak deflection is smaller than the second peak deflection, whereas in case 2 (the mass is moved towards the clamped end) the first peak deflection is larger than the second peak deflection. In both cases, the first and second peak deflections increase with increase in mass and decrease with increase in mass travelling time.

The difference between the transient deflection (first and second peak deflections) and the steady state ($T \geqslant T_t$) vibration amplitude in case 1 is related to the mass travelling time T_t. For $T_t = 5$ in case 1, the transient deflection is smaller than the steady state vibration amplitude (Figures 3 and 4). However for $T_t = 8$, the transient deflection is larger than the steady state vibration amplitude (Figure 5). In case 2 the transient deflection is always larger than the steady state vibration amplitude (Figures 6–8).

The effects of mass N and mass travelling time T_t on the steady state vibration amplitude of the beam under the moving mass for cases 1 and 2 are best illustrated in Figure 9. Comparison of the steady state vibration amplitude in both cases show that the steady state vibration amplitude of case 1 is greater than that of case 2 for the same mass and travelling time. This can be expected that when the mass is more close to the clamped end, the vibration amplitude will be reduced. In case 1 for $T_t = 5$ and 6 the steady state vibration amplitude increases with increase in mass N. In case 2 for $T_t = 5$ the steady state vibration amplitude decreases as N increases, whereas for $T_t = 6$ an increase in moving mass N causes an increase in the steady state vibration amplitude. In both cases for $T_t = 7$

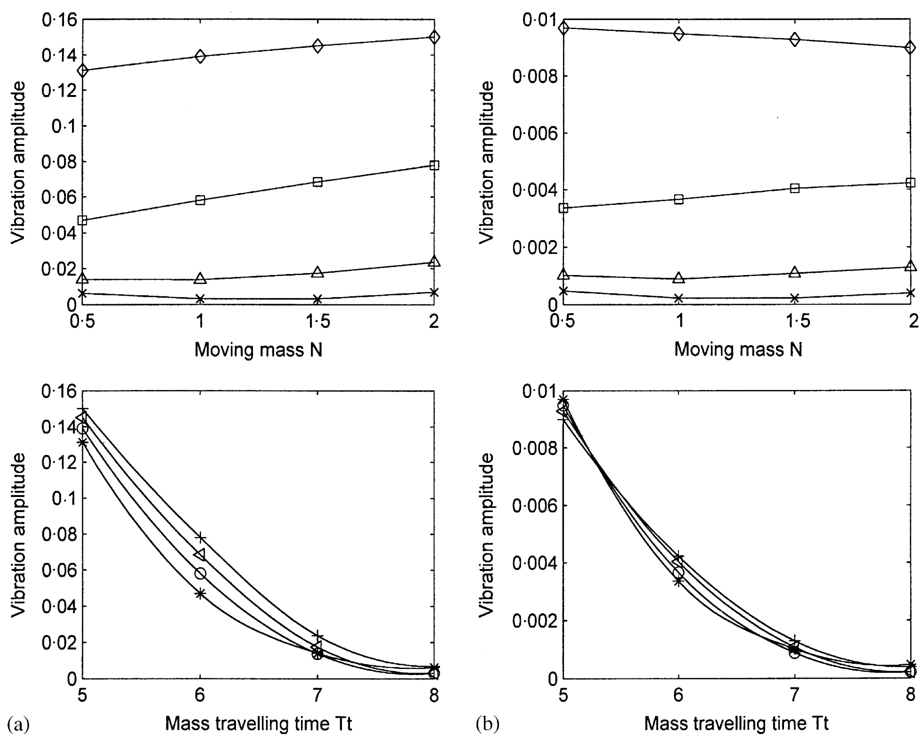

Figure 9. Steady state vibration amplitude of beam as function of moving mass N and mass travelling time T_t. Values of mass travelling time T_t: $-\Diamond-$, $T_t = 5$; $-\Box-$, $T_t = 6$; $-\triangle-$, $T_t = 7$; $-\times-$, $T_t = 8$. Values of moving mass N: $-*-$, $N = 0{\cdot}5$; $-\bigcirc-$, $N = 1{\cdot}0$; $-\triangleleft-$, $N = 1{\cdot}5$; $-+-$, $N = 2{\cdot}0$. (a) case 1; (b) case 2.

and 8 the steady state vibration amplitude decreases first and then increases with increase in mass N. However, a decrease in the mass travelling time T_t causes an increase in the the steady state vibration amplitude under all conditions in both cases.

The deflection of the beam under the moving mass without considering the centrifugal stiffening effect [by setting $P(r, t) = 0$ in equation (5)] is shown with dotted line in Figures 3–8. It can be seen that the existence of the centrifugal stiffening effect can reduce the steady state vibration amplitude. If the centrifugal stiffening effect is ignored in the simulation, the computed steady state vibration amplitude will be increased. The increase percentage is found to range from about 6% in Figures 3 and 6 to about 16% in Figures 5 and 8.

In this paper, the eigenfunctions of a non-rotating cantilever beam are used as the basis functions and a three-mode approximation is used in the deflection equation (10). Simulation results using MATLAB show that $v(s_0, T)$ is dominated by the first mode, and the contributions of the second and third modes are very small. This suggests that the difference between the three-mode approximation and the approximation using more modes is insignificant.

5. CONCLUSIONS

In this paper, the dynamic response of a flexible arm rotating in a horizontal plane and carrying a moving mass is studied. The arm is modelled by the Euler–Bernoulli beam theory. The equation of motion is derived using the assumed mode method in conjunction with Hamilton's principle. The effect of centrifugal stiffening due to the rotation of the beam is taken into account in the analysis. The trajectory inputs of the hub angle and the moving mass are simulated using prescribed cosine profiles. The equation of motion is solved numerically using the fourth order Runge–Kutta method. The results are presented graphically to show the influence of the centrifugal stiffening effect, different moving mass, mass travelling time and trajectory profiles on the deflection of the beam.

REFERENCES

1. R.-T. Wang and T.-H. Chou 1998 *Journal of Sound and Vibration* **218**, 117–131. Non-linear vibration of Timoshenko beam due to a moving force and the weight of beam.
2. M. Abu Hilal and H. S. Zibdeh 2000 *Journal of Sound and Vibration* **229**, 377–388. Vibration analysis of beams with general boundary conditions traversed by a moving force.
3. G. Visweswara Rao 2000 *Transactions of the American Society of Mechanical Engineers, Journal of Vibration and Acoustics* **122**, 281–289. Linear dynamics of an elastic beam under moving loads.
4. E. Esmailzadeh and M. Ghorashi 1995 *Journal of Sound and Vibration* **184**, 9–17. Vibration analysis of beams traversed by uniform partially distributed moving masses.
5. M. A. Foda and Z. Abduljabbar 1998 *Journal of Sound and Vibration* **210**, 295–306. A dynamic Green function formulation for the response of a beam structure to a moving mass.
6. Seroj Mackertich 1990 *Journal of the Acoustical Society of America* **88**, 1175–1178. Moving load on a Timoshenko beam.
7. G. Michaltsos, D. Sophianopoulos and A. N. Kounadis 1996 *Journal of Sound and Vibration* **191**, 357–362. The effect of a moving mass and other parameters on the dynamic response of a simply supported beam.
8. H. P. Lee 1996 *Journal of Sound and Vibration* **191**, 289–294. Dynamic response of a beam with a moving mass.
9. S. A. Q. Siddiqui, M. F. Golnaraghi and G. R. Heppler 1998 *Nonlinear Dynamics* **15**, 137–154. Dynamics of a flexible cantilever beam carrying a moving mass.
10. M. M. Stanisic 1985 *Ingenieur-Archiv* **55**, 176–185. On a new theory of the dynamic behavior of the structures carrying moving masses.

11. F. Khalily, M. F. Golnaraghi and G. R. Heppler 1994 *Nonlinear Dynamics* **5**, 493–513. On the dynamic behaviour of a flexible beam carrying a moving mass.
12. S. Park and Y. Youm 2001 *Journal of Sound and Vibration* **240**, 131–157. Motion of a moving elastic beam carrying a moving mass — analysis and experimental verification.
13. E. H. K. Fung and D. T. W. Yau 2001 *Journal of Sound and Vibration* **241**, 857–878. Vibration frequencies of a rotating flexible arm carrying a moving mass.
14. E. H. K. Fung and D. T. W. Yau 1999 *Journal of Sound and Vibration* **224**, 809–841. Effects of centrifugal stiffening on the vibration frequencies of a constrained flexible arm.